culated using the corrected convergence angle as: $Q_c = (\pi + 2\tan^{-1}d/r)r^2v$ (Fig. A). *Results:* Without AW Q correlated closely with Q_t ($r = 0.95$ $p < 0.005$ $Q/Q_t = 1.03 \pm 0.08$). However, with an AW velocity-distance profiles were shifted right and upward (Fig. B) leading to significant overestimation of Q_t ($Q/Q_t = 1\ 50 \pm 0.53$). Using the convergence angle function almost completely corrected this overestimation with $Q_c/Q_t = 1.06 \pm 0.25$. *Conclusion:* 1) AW caused significant overestimation of Q calculated by PFC. 2) Adjusting the convergence angle as a function of wall distance and velocity contour almost completely corrected the overestimation. 3) This algorithm is suitable for automatization and will improve the application of PFC in a wider range of clinical situations.

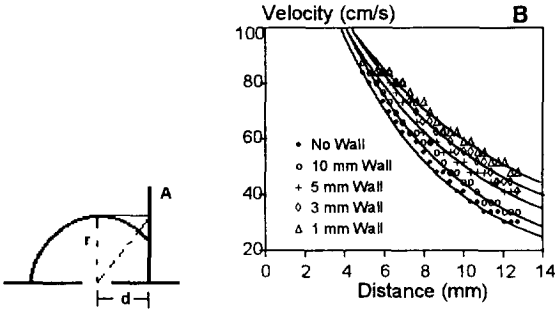

11:15

747-4 Evaluation of Regurgitant Jets by Sound Intensity Using a Pulsatile Flow Model: Potential Contribution of Regurgitant Volume and Reynolds Number

Marieke J.H. Baars, Dymph K. Aaftink, Arnaldo Passafini, Antoinette Kenny, Takahiro Shiota, David J. Sahn. *Oregon Health Sciences Univ, Portland, OR*

Our goal in this study was to determine whether a new type of digital heart sound analysis method could give quantitative information about flow velocity and volume so as to allow a potentially lower-cost approach to followup studies of patients with stenotic or regurgitant valve lesions. To elucidate the relationships between hydrodynamic factors such as Reynolds number, flow velocity and flow volume and the sound characteristics of cardiac murmurs, we developed an in vitro pulsatile flow model with variable orifice size and shape (circular 0.11 cm^2, 0.24 cm^2, 1.77 cm^2 and 3.80 cm^2; oval 0.24 cm^2, with a ratio of major to minor axis = 2; rectangular 0.24 cm^2, ratio = 4). Heart sounds were recorded with a new digital system (MCG) with real time spectral analysis and display and averaged over 15 "cardiac" cycles. Mean flow rate ranged from 0.6 l/min to 6 l/min. Actual instantaneous flow rate was measured using an ultrasonic flow meter for peak flow rates 1.6 l/min to 16.8 l/min. Reynolds number ranged from 6820 to 40050. For each orifice, there was an excellent relationship between total integrated sound energy (See figure: integration of intensity (I) and frequency (F) over time (T).) obtained by digital processing and Reynolds number, peak flow velocity and peak flow rate ($r = 0.89$–0.97, 0.89–0.97, 0.93–0.99, $p < 0.001$, respectively). The best relationship was obtained for the smallest orifice. Higher sound energies were detected for any given flow volume in asymmetrical orifices, probably due to higher turbulence. For all orifices combined, a correlation was found between peak frequency and peak velocity, but only *total sound energy* was correlated with peak flow rate ($r = 0.84$, $p < 0.01$). Total integrated sound energy determined digitally is related to peak flow rate; peak velocity and Reynolds number parallel peak sound frequency.

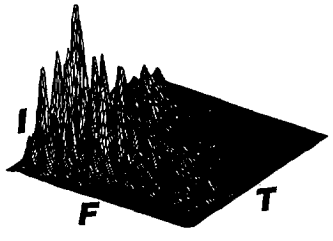

11:30

747-5 Transesophageal Echocardiographic Quantitation of Mitral Leaflet Thickness in Patients with Mitral Valve Prolapse

Eric K. Louie, David Langholz, William J. Mackin, Diane E. Wallis, William R. Jacobs, Patrick J. Scanlon. *Loyola University Medical Center, Maywood, IL*

Mitral leaflets which appear abnormally thick by *transthoracic* echo predict an adverse prognosis in pts with mitral valve prolapse (MVP). While it is known from pathologic studies that the valve tissue in such pts is both redundant and abnormally thick, the echocardiographic appearance of increased thickness may result from a combination of overlap of redundant tissue and intrinsic increases in leaflet thickness. *Transesophageal* echo (TEE) affords the opportunity to more precisely characterize the morphology of the mitral leaflets in these patients. Accordingly, twenty-two pts [11 with MVP (defined as superior displacement of the mitral leaflets above the mitral annulus on the parasternal long axis view of the transthoracic echo and increased diastolic width of the anterior mitral leaflet) and 11 controls (CTRL)] prospectively underwent detailed TEE examination to quantify mitral leaflet thickness. Since systolic tensing of the closed mitral leaflets minimizes tissue overlap, systolic leaflet width was used to measure intrinsic tissue thickness. In contrast, the width of the relatively slack mitral leaflets in diastole represents a combination of both leaflet overlap and intrinsic tissue thickness. Blinded TEE measurements of leaflet width demonstrated greater *diastolic* width of both anterior (0.64 ± 0.20 v. 0.30 ± 0.04 cm, $p < 0.001$) and posterior (0.67 ± 0.39 v. 0.31 ± 0.06 cm, $p < 0.01$) leaflets in MVP compared to CTRL. In contrast *systolic* width of the anterior (0.22 ± 0.05 v. 0.20 ± 0.04 cm, NS) and posterior (0.25 ± 0.07 v. 0.24 ± 0.05 cm, NS) leaflets were similar in MVP and CTRL. Fractional change in leaflet width from diastole to systole ($\%\Delta W$ = [(diastolic width) − (systolic width)] × 100/[diastolic width]) was measured as an index of the change in leaflet overlap between diastole and systole, $\%\Delta W$ was significantly greater for both anterior (62 ± 13 v. $34 \pm 16\%$, $p < 0.001$) and posterior (54 ± 19 v. $22 \pm 21\%$, $p < 0.005$) leaflets in MVP compared to CTRL. *Conclusions:* In MVP the echocardiographic appearance of increased diastolic mitral leaflet thickness is largely due to tissue overlap of the redundant leaflets, while they are relatively slack. By contrast under systolic tensioning, which minimizes tissue overlap, the leaflet thickness appears similar in MVP pts and CTRL.

11:45

747-6 Myocardial Blood Flow in Aortic Regurgitation: Comparison of Global and Regional Blood Flow to Regional Wall Stresses

Edmund M. Herrold, Steven M. Goldfine, Norman M. Magid, Jeffrey S. Borer. *Cornell Medical Center, New York, NY*

The impact of regional wall stress (WS) abnormalities on regional coronary flow (CBF) in aortic regurgitation (AR) is not known. However, the existence of such a relation is of potential importance since it might account in part for LV dysfunction and myocardial fibrosis seen in AR, and could suggest therapeutic strategies. We have previously developed and validated a method for calculating regional WS in the radial, circumferential and meridional directions from mid wall (MW) to apex (AP) and endocardium (ENDO) to epicardium (EPI) using a 4000 element model of the LV. To define the relation of regional WS and CBF in AR, we applied our LV model in 5 normal (NL) and 4 AR rabbits in which regional CBF was measured using fluorescent microspheres. CBF and radial WS were as follows:

		CBF (ml/min/gm)		Radial WS ($\times 10^3$ dynes/cm^2)	
		MW	AP	MW	AP
NL	EPI	2.49	1.30	83	29*
	ENDO	2.09	0.74	133	133*
AR	EPI	1.82	1.82*	86	38*
	ENDO	1.41	0.77*	133	133*

* = $p < 0.001$ (EPI vs ENDO for CBF, EPI to ENDO gradient in AR vs NL for radial WS)

Thus, in AR, transmural CBF distribution varies significantly at the apex, while this tendency is less marked and less consistent in NL. No discernable transmural variation was apparent elsewhere in either group. These differences paralleled inversely the transmural variations in radial WS in AR vs NL. In contrast, meridional WS and circumferential WS were uniformly and significantly higher in AR than NL at apex and base (all $p < 0.001$), a pattern which bore no relation to regional CBF pattern. Thus, regional radial WS influences regional transmural CBF pattern in AR. The importance of this relation to regional LV function and regional myocardial fibrosis in AR now must be assessed.